TESTING THE EFFICACY OF ELECTRICAL CONDUCTIVITY AS AN INDICATOR OF URBAN WATERSHED DISTURBANCE

by

EMILY M. JOHNSON

(Under the Direction of SETH WENGER AND AMY ROSEMOND)

ABSTRACT

Elevated streamwater conductivity is a symptom of watershed urbanization and is correlated with degraded water quality and impaired biotic assemblages. Stormwater runoff, sewage effluent, and sediment inputs are potential sources of ions that drive conductivity. Using in-situ and real-time remote monitoring technologies, we monitored specific conductance (SPC), stage height, and temperature over periods from July 2015 to January 2018 across an urbanization gradient in Athens, GA, USA. Water chemistry was measured at baseflow and elevated SPC conditions. Baseflow SPC was variable spatially among sites and temporally within sites. Normalized daily patterns in SPC were different in urban vs rural and suburban sites. Cross correlation of SPC and stage height revealed distinct stormwater first flush signals, and peak SPC was associated with elevated nitrogen concentrations at urban sites, consistent with sewage inputs. Continuous, real-time monitoring of SPC can be a useful management tool for identifying and diagnosing pollution events in urban watersheds.

INDEX WORDS: specific conductivity, urban stream syndrome, real-time monitoring, sewage, stormwater, first flush

TESTING THE EFFICACY OF ELECTRICAL CONDUCTIVITY AS AN INDICATOR OF URBAN WATERSHED DISTURBANCE

by

EMILY M. JOHNSON

BS, Kansas State University, 2016

A Thesis Submitted to the Graduate Faculty of The University of Georgia in Partial Fulfillment of the Requirements for the Degree

MASTER OF SCIENCE

ATHENS, GEORGIA

2020

TESTING THE EFFICACY OF ELECTRICAL CONDUCTIVITY AS AN INDICATOR OF URBAN WATERSHED DISTURBANCE

by

EMILY M. JOHNSON

Major Professor:	SETH WENGER
	AMY ROSEMOND
Committee:	LAURIE FOWLER
	JOHN DOWD

Electronic Version Approved:

Ron Walcott
Interim Dean of the Graduate School
The University of Georgia
May 2020

DEDICATION

This work is dedicated to John Spencer and his family. Although I did not have the privilege of knowing John for long, my life has forever been impacted by his passion for ecology and the legacy he left at the Odum School of Ecology. His foundational work was the impetus for this project.

ACKNOWLEDGEMENTS

I would first and foremost like to thank the friends and family of John Spencer, who funded the John Spencer Fellowship, which allowed me to pursue this research and my goals of working in applied freshwater science. I would also like to thank my graduate advisors, Seth Wenger and Amy Rosemond, for their support both academically and personally throughout my time at UGA. Each has provided me with invaluable guidance through challenges in my studies and life, and I am grateful for their expertise and compassion. Additionally, I would like to thank my committee members, John Dowd and Laurie Fowler, for their guidance and perspective in the development of this project. Very special recognition should be given to Phillip Bumpers and Paige Miller, who were vital in the planning and execution of field and analytical methods for this work. They, along with all of my lab mates in the River Basin Center, also provided valued friendship and emotional support over the years.

TABLE OF CONTENTS

Page

ACKNOWLEDGEMENTS v

LIST OF TABLES viii

LIST OF FIGURES x

CHAPTER

1 INTRODUCTION 1

2 METHODS 6

Study area 6

Sampling Period 1: Characterization of trends in SPC 6

Development of real-time monitoring stations 7

Sampling Period 2: Hypothesis testing 8

3 RESULTS 14

Sampling Period 1: Characterization of trends in SPC 14

Sampling Period 2: Hypothesis testing 15

4 DISCUSSION 28

Conductivity as a monitoring metric 28

Drawbacks of continuous monitoring techniques 30

Future considerations 31

REFERENCES 32

LIST OF TABLES

Page

Table 1: Characterization of each site by stream name, GPS location (Latitude, Longitude), percent urbanization (% Urban), sampling duration, percent of forest cover (% Forest), percent of pasture cover (% Pasture) and drainage area in km^2. Sampling Period 1 refers to sites where data was collected from July 2015 to April 2016. Sampling Period 2 refers to sites where data was collected from October 2016 to January 2018................11

Table 2: Target conditions for in0lab turbidity trials. All values are reported in Nephelometric Turbidity Units (NTU) where "Start NTU" is the turbidity conditions at the beginning of each trial, "Addition X" is the targeted total turbidity following the first, second, or third sediment addition, and "End NTU" is the final total turbidity desired for each trial. 12

Table 3: Summary of in-stream conditions at each site. Readings for specific conductivity (μS $cm^{-1)}$, stage height (meters), and temperature (degrees Celsius) were taken every 5 minutes using in-situ data loggers. Mean (standard deviation), minimum (Min), and maximum (Max) recorded values were summarized over the total sampling duration at each site. Sampling periods for each site are outlined in Table 1. Data was cleaned prior to analysis by excluding known logger errors, including erroneous measurements, improper installation of loggers, and periods of logger inactivity. 17

Table 4: Mean (standard deviation) of water chemistry data collected during Sampling Period 1. Samples were collected in June and October 2015 at all sites except S2, which does not have data for this sampling period. S2 was added to the study during Sampling Period 2 to reflect management priorities, as stated by the Athens-Clarke County Transportation and Public Works Department (ACC TPWD). Units are reported in mg L^{-1} unless otherwise noted. Sites are listed left-to-right in order of increasing percent

imperviousness as defined in Table 1. *The number of samples analyzed equals two in all cases except for site R1 analyte PO4, which is represented by a single data point due to likely contamination during analysis of the October 2015 sample. 18

Table 5: Minimum, maximum, and mean (standard deviation) of stormflow SPC aggregated by imperviousness and site for all identified storm events. Stormflow SPC was determined by identifying the SPC value recorded 20 minutes prior to the start of a precipitation event. The change in SPC from baseflow during storm events (ΔSPC) was calculated by subtracting the mean SPC value for stormflows from the mean SPC value during baseflow prior to storm events. The sampling period for each site is outlined in Table 1. The number of storm events assessed varies by site and ranges from 85-284 events. In all cases, ΔSPC is positive, which represents an increase in SPC during stormflows, and the largest ΔSPC values occur at the more urbanized sites. All values are reported in μS cm^{-1}. 19

Table 6: Summary of water chemistry data collected from January to August of 2018. Samples were automatically collected during high SPC conditions at rea-time remote monitoring stations. WE calculated mean (standard deviation) of nutrient and ion concentrations at each site, then determined the ratio of mean ionic concentrations at peak SPC conditions compared to mean ionic concentrations at baseflow SPC conditions. Ratio values greater than 1 indicate higher concentrations at peak SPC conditions, while values less than 1 indicate higher concentrations at baseflow SPC conditions. For example, peak calcium (Ca) concentration was 1.21x higher than baseflow concentrations at U3 but was 0.83x lower than baseflow concentrations at U4. 20

Table 7: Readings of SPC taken at the start, end, and every 5 minutes during turbidity trials. Conditions for each trial are listed in Table 2. 20

LIST OF FIGURES

Page

Figure 1: Map of all sampling sites and subbasin land cover based on the 2008 Georgia Land Use Trends database from the University of Georgia Natural Resources Spatial Analysis Lab. Red colors represent developed land and green colors represent natural/forest cover. All sites were within Athens-Clarke County, GA (USA). Sites were selected across a gradient of urbanization and forest cover. 13

Figure 2: Complete time series of SPC readings taken at each of the 10 sites. Line colors correspond to classification of sites based on urbanization categories. Green represents rural sites, blue represents suburban sites, and red represents urban sites. 21

Figure 3: Normalized daily trends of SPC based on continuous data collected at five-minute intervals at each site. Variation from the mean value is on the y-axis and hour of the day is on the x-axis. The x-axis is represented in a 24-hour time scale, where 0-24 represents the time between 12:00AM to 11:59PM. 22

Figure 4: Heat map of correlation between nutrients and ions across all baseflow water chemistry samples at all sampled sites. Two baseflow water chemistry samples were collected at each site during Sampling Period 1 (Table 1), where the first and second samples were collected in June and October 2015, respectively. The size of each dot represents the slope, or strength, of the correlation between the two intersecting analytes, while the color represents the positivity or negativity of the relationship where more intense colors were more positive or negative than dull colors. 23

Figure 5: Cross correlation of SPC and stage height at each site. The y-axis represents the strength and positivity or negativity of the relationship between SPC and stage height, while the x-axis represents the number of time lags (k), where a single time lag equals

10 minutes. For example, a lag of +5 refers to the correlation between x (stage height) and time t_0+5 (t_0+50 minutes) and y (SPC) at time t_0. 24

Figure 6: Heat map of correlation between nutrients and ions across all samples collected at sites S2, U3 and U4 using automated water chemistry sampling. Samples were collected from January to August 2018. The size of each dot represents the slope, or strength, of the correlation between the two analytes, while the color represents the positivity or negativity of the relationship. The intensity of the color represents the relative positivity or negativity of the relationship, with more intense colors being more positive or negative than dull colors. 25

Figure 7: Boxplot of ionic concentrations at site U3 comparing water chemistry of samples taken at baseflow to that of samples taken during peak SPC conditions. Concentration of analytes is represented on the y-axis where the scale on each plot is adjusted to encompass the range of variability for each analyte. Boxes represent the median and first and third quartiles while whiskers represent the minimum and maximum. 26

Figure 8: Boxplot of ionic concentrations at site U4 comparing water chemistry of samples taken at baseflow to that of samples taken during peak SPC conditions. Concentration of analytes is represented on the y-axis, where the scale on each plot is adjusted to encompass the range of variability for each analyte. Boxes represent the median and first and third quartiles while whiskers represent the minimum and maximum. 27

CHAPTER 1

INTRODUCTION

Introduction

Over half of the global population lives within urban areas, and the number of urban inhabitants is expected to continue to increase (Cohen 2006). This expansion and intensification of urbanization leads to significant changes in the form and function of nearby rivers and streams due to a variety of physical, chemical and biological pathways (Walsh et al., 2005; Wenger et al., 2009). While the specific drivers of watershed urbanization, as well as in-stream responses, can vary in different physiographic regions and with climate, streamwater conductivity (measured as specific conductance, SPC), is a robust indicator of the effects of urbanization on water quality (Booth et al. 2016). SPC can be elevated due to a variety of stressors associated with watershed disturbance, including inputs from sewage, sediment, road salting, and transportation infrastructure (Anderson et al. 2004, Daley et al. 2009, Kaushal et al. 2018). With improved technology and lower cost of sensors, SPC can now be measured at greater spatial and finer-resolution temporal scales (Baker et al. 2019), creating new capacity for adoption as a management tool.

The potential for access to SPC data provides new opportunities for watershed and water quality managers to track pollutants. Managers associated with municipalities may find SPC data useful, as they must meet state and federal water quality standards in order to remain in compliance with permits for discharges from critical infrastructure, such as stormwater and wastewater systems (40 C.F.R. § 122.21 (2015)). Managers regularly monitor water quality and address sources of pollution that cause water bodies to fall below regulatory standards. Traditional techniques used for monitoring water quality, which typically involve periodic site visits to collect instantaneous physical and chemical data (Grayson et al., 1997), are useful to confirm or identify chronic and point-source pollution and describe 'typical' conditions in watersheds. Unfortunately, this type of sampling often misses episodic disturbances from acute stressors. Thus, we lack an understanding of how water quality in urban settings changes on fine temporal scales in response to episodic urban disturbances.

Specific conductivity data can potentially assist water quality managers in identifying both chronic and acute pollution events in urban streams. Conductivity is relatively easy to measure using a variety of techniques and technologies (Moore et al., 2008) and has been strongly correlated with stressors such as total dissolved solids (Fenn 1987) and elevated nutrients (Morgan et al., 2006). In addition, SPC is an excellent indicator of biotic impairment (Wenner et al., 2003; Sterling et al. 2016). However, traditional techniques for monitoring conductivity, which involve periodic site visits to collect instantaneous data (Grayson et al., 1997), typically only provide information on baseline watershed conditions. Exceptions include storm sampling programs which use targeted collection methods during rain events in order to assess the quality and chemical makeup of stormwater runoff from impervious surfaces (Deletic 1998; Sansalone et al., 2005; Flint & Davis, 2007). However, even accounting for these targeted storm sampling programs, we frequently lack an understanding of how conductivity changes over time during episodic and acute disturbances that are common in urban settings. Our study aims to characterize fine-scale temporal trends in conductivity and explore the efficacy of continuous monitoring for management purposes.

While many studies have related changes in conductivity to specific urban stressors, few studies have attempted to identify specific stressors associated with fine resolution temporal patterns in conductivity. In this study, we explored three pattern-stressor relationships. The first was the first flush effect (FFE) of stormwater runoff, which is well documented in urban areas and is characterized by an increased concentration of pollutants in runoff during the onset of a rain event. Several studies have found that FFE is associated with elevated SPC in urban streams (U.S. EPA 1996; Deletic 1998; Sansalone et al., 2005; Flint & Davis 2007). Therefore, we hypothesized that corresponding increases in SPC and stage height are indicative of stormwater runoff entering the stream from the surrounding landscape. Conductivity in streams affected by FFE tends to be elevated during the onset of a storm in correlation with the highest concentrations of total dissolved solids (TDS) and total suspended solids (TSS) (Deletic 1998; Sansalone et al., 2005). However, these relationships are typically documented with laborious storm sampling protocols, where managers must opportunistically collect runoff samples by hand during the beginning of a rainfall event. This type of sampling, similar to other traditional protocols, are challenging, time consuming and costly to perform across a broad spatial scale. Continuous monitoring of EC could potentially reduce the need for storm sampling in order to identify FFE in urban streams.

Another well-documented source of pollution in urban landscapes is sewage and septic waste. Concentrations of many ions, as well as SPC, tend to be elevated in systems known to receive combined sewer overflows (CSOs) and sewage effluent (Rose 2002; Hatt et al., 2004; Rose 2007). In the Piedmont region of northern Georgia (USA), one study showed that HCO_3^-, Cl^-, SO_4^{2-} concentrations and EC in basins characterized by close proximity to sewage trunk lines and known CSOs were up to 4x elevated when compared to other urban drainages (Rose 2007). Similar results have been recorded in other countries (Bondarenko et al., 2016), showing the global applicability of SPC as an indicator of pollution from sewage. In practice, sewer leaks can be difficult to identify and locate, and some leaks may go undetected for extended periods of time. Continuous monitoring of SPC at a broad scale could assist managers in the identification of sewage leaks into streams and enhance management programs which aim to detect, diagnose and eliminate sewer leakage. In our study area, unlike areas that experience CSOs, the wastewater infrastructure is separate for storm and sewage. This separate system makes it unlikely that we would observe sewer leaks in conjunction with storm events. However, aging infrastructure and close proximity of sewer lines to streams creates high potential for sewer leaks to occur. We predicted that sewer leaks which occur during times of elevated stress on the system (i.e. high usage of sewage infrastructure) would release pulses of wastewater carrying high concentrations of ions. Therefore, we hypothesized that changes in SPC which occur in the form of regular, nonrandom patterns that are not associated with changes in stage height are indicative of sewer leaks. We also tested whether particular ions (e.g., NO_3, Na) that would be indicators of sewage inputs were elevated with SPC.

A third urban stressor is sediment inputs into streams, which is commonly measured as suspended sediment or turbidity. Increased turbidity is a common symptom of urbanization that is associated with impaired biotic condition and ecosystem function (Paul & Meyer 2001; Walsh et al., 2005; Wenger et al., 2009). The primary source of elevated sediment in many urban streams is erosion from land-disturbing activity in the watershed, although channel erosion and legacy sediment can also be important sources. In one study, erosion in urban areas experiencing active construction resulted in total suspended sediment concentrations of 3,000 to 150,000 mg/L, while nearby natural and agricultural catchments rarely exceeded 2,000 mg/L (Wolman & Schick 1967). In Georgia, the Erosion and Sedimentation Control Act (ESCA) was developed to limit the load of sediment in streams and protect state waters from excess erosion and sedimentation from land disturbing activities. The ESCA mandates that best management practices (BMPs) must be implemented for all land disturbing activities, and that those BMPs must control any discharge from the disturbed area sufficiently so that turbidity does not increase by more than 25 NTUs. Given that SPC integrates ions associated with surrounding geology and urban pollutants, and that turbidity reflects increased runoff of urban soils, it is possible that continuous monitoring of SPC could reveal patterns attributable to sediment inputs. Therefore, we hypothesized that apparently random and irregular fluctuations in SPC are indicative of sediment inputs. This has potential applications for monitoring land disturbing activity and identifying regulatory violations.

Development of real-time remote monitoring (RTRM) (Glasgow et al., 2004) technology has solved many of the challenges associated with traditional sampling methods and allowed for an improved understanding and management of river systems using high temporal resolution data (Hart and Martinez, 2006; Kotomaki et al., 2009; O'Flynn et al., 2010). RTRM has also been shown to be valuable in monitoring of water quality and compliance with environmental standards (Kotomaki et al., 2009; Eidson et al., 2010; O'Flynn et al., 2010). Across the United States, RTRM networks have been implemented by the United States Geological Survey (USGS) to monitor precipitation, discharge, water temperature, and in some cases streamwater conductivity (USGS 2020). Recently, increased availability of low-cost sensors and microcontrollers has encouraged the development and testing of custom-built RTRM systems. This "do-it-yourself" (DIY) approach allows for more specific and focused data collection at a lower cost than stock multi-sensor systems. Additionally, RTRM can be integrated with diagnostic systems that provide risk-alert strategies for environmental conditions that may pose risks to human health, such as flooding (Ancona et al., 2014). Using this technology for the continuous monitoring of EC could potentially assist in management decision making for assessing multiple pollutants.

The goals of this study were to characterize fine-scale temporal patterns of SPC across a spatial gradient of urbanization and to test the efficacy of real-time, continuous monitoring of SPC as a tool for diagnosing watershed disturbance in cooperation with the Athens-Clarke County Transportation & Public Works Department (ACC TPWD). We predicted that by continuously tracking SPC, we could distinguish between stressors which episodically enter the system via runoff and those which are chronic. Specifically, we hypothesized that 1) urban sites would display positive relationships between SPC and stage height indicative of the FFE, 2) sites impacted by sewer leaks would display changes in SPC which diverge from stage height in regular, nonrandom patterns, and 3) random and irregular fluctuations in SPC independent of stage height would be indicative of sediment inputs.

CHAPTER 2

METHODS

Study area

This study took place in the Piedmont physiographic region of northeast Georgia (USA), which is characterized by red clay soils and basins are underlain by aluminosilicate rock (Drever 1997). Stream water ions are dominated by Ca^{2+}, Na^{+}, and HCO_3^- from mineral weathering (Drever 1997; Rose 2002; Griffith 2014). Urban streams in the Piedmont have been shown to contain elevated concentrations of Ca^{2+}, Na^{+}, HCO_3^-, Cl^-, and SO_4^{2-}, producing elevated SPC (Rose 2002; Rose 2007).

All study sites were located in Athens-Clarke County within the upper Oconee River Basin (Figure 1). We collected data in ten 2nd and 3rd order tributaries across a gradient of urbanization (5.53-99.05 % urban).We delineated the catchment above each site and calculated the percentage of forested, agricultural, and developed land uses using the Georgia Land Use Trends dataset from the University of Georgia Natural Resources Spatial Analysis Lab. After calculating the percentage of each major land use in each of the ten study catchments, we categorized sites based on the % of urban land use where four sites were categorized as urban (> 50% urban), three sites were suburban (25-49% urban), and three sites were forested (0-24% urban) (Table 1).

Sampling Period 1: Characterization of trends in SPC

To identify unique patterns of specific conductivity (SPC) that may be attributed to urban stressors, we first had to understand how SPC varied at fine temporal scales. We collected SPC, stage height and temperature at each site at five-minute intervals using in-situ data loggers (Onset Computer Corporation, Bourne, Massachusetts) from July 2015 to April 2016 at all sites except R1, S2 and U4 (Table 1, Sampling Period 1). To establish a baseline relationship between water chemistry and SPC at each site, we collected grab samples in June and October 2015 at all sites except S2. Sites R1, S2 and U4 were added to this study during Sampling Period 2 to reflect priorities of local managers, as described in the following section "Development of real-time monitoring stations."

For each site, temperature, SPC and stage height data were characterized by mean, standard deviation (SD), daily minimum and daily maximum. For stage height, we excluded known probe errors, which occurred in the data as negative water level observations. We characterized patterns in SPC at each site over a 24-hour period to test for differences in diel, or daily, patterns among streams. To do so, we sorted continuous SPC data by site and hour of the day, resulting in mean hourly SPC values at each site. These mean hourly SPC data were then plotted over a 24-hour period and plots were smoothed using a general additive model with a cubic spline. We calculated the normalized SPC by subtracting the mean and then dividing by the standard deviation of each site. To quantify the similarity in daily patterns of SPC at each site, we analyzed the correlation between all sets of daily smoothed, normalized SPC signals using the diss function in the R package TSclust (Montero and Vilar 2014). We then performed hierarchical clustering on the correlation dissimilarity matrix to identify patterns among different daily signals using the R function hclust with the complete linkage method (R Core Team 2018).

Water chemistry data were analyzed by taking the mean and standard deviation of nutrients and major ions at each site. We then tested for relationships between SPC and each nutrient and ion by calculating the Pearson correlation coefficient using the R function cor.

Development of real-time monitoring stations

To test the management applications of continuous SPC monitoring, we built three custom monitoring stations which measured continuous SPC, stage height, and temperature at five-minute intervals using HYDROS 21 sensors (Meter Group, Inc., Pullman, WA). For each station, the sensor was connected to an Arduino-compatible Mbili microcontroller (SODAQ, Hilversum, Netherlands), which relayed the raw data to our servers via a cellular data uplink using a GPRSbee communications expansion board (SODAQ, Hilversum, Netherlands). Stations were deployed at Trail Creek, Brooklyn Creek and Tanyard Creek, which were selected based on accessibility and management priority, as determined by local managers with the ACC TPWD.

Sampling Period 2: Hypothesis testing

Hypothesis 1 - FFE

To test the FFE hypothesis, we conducted a second round of field measurements, recording SPC, stage height and temperature continuously at five-minute intervals across a gradient of urbanization using the same in-situ data loggers (Onset Computer Corporation, Bourne, Massachusetts). Data collection occurred from October 2016 to January 2018 at all sites except Tallassee Creek, McNutt Creek, and Brickyard Creek (Table 1, Sampling Period 2). We obtained archived precipitation data for our study period from the University of Georgia Weather and Climate Research Laboratory.

We used two approaches to test the ability of SPC to capture a first flush effect. First, for every day during which precipitation was recorded, we identified the maximum SPC value recorded at each site, under the hypothesis that this represented the first flush peak. We compared this value to the mean SPC in the 20-minute period prior to the peak (not counting the reading just before the maximum), which we called baseflow SPC for this purpose. We subtracted baseflow SPC from stormflow SPC to get a change in SPC (ΔSPC) for the first flush of rain events.

Secondly, we characterized the relationship between SPC and stage height with cross correlation function (CCF) analysis of the time series for each site. The time series used in the cross-correlation analyses were constructed by binning and averaging SPC and stage height data into 15-minute intervals to account for differences in the timing of the 5-minute collection intervals for each probe. To satisfy the stationarity assumption for conducting cross-correlation analyses (i.e., variables at time t, x_t, are not related to variables at time *t-1*, *t-2*, etc.), we firstdifferenced each time series (i.e., $x_{t+1} - x_t$) (Hyndman and Athanasopoulos 2018). We interpreted sample cross-correlation analyses of SPC (x_t) and stage height (y_t) by assessing the correlations between x_{t+h} and y_t for $h = 0, \pm 1, \pm 2, \pm 3$ and so on. A significant correlation between x_{t+h} and y_t for a positive h means that x lags y (or y leads x). We expected SPC to lag behind stage height by approximately one to two lags (15-30 minutes) due to the delay between the onset of a storm and the timing of runoff entering the stream which is attributed to varied distance of overland flow and length of stormwater infrastructure at each site. All calculations were computed using the statistical package R 3.4.3 (R Core Team 2004).

Hypothesis 2 - sewage

To test for relationships between SPC and sewer leaks, we collected water chemistry samples at sites S2, U3 and U4 during baseflow and peak SPC conditions. These samples were collected using a custom-built automated peristaltic pump system powered by the real-time monitoring station at each site. Sample collection was triggered by site-specific threshold SPC values. Threshold values were based on the third quartile range of each site and reflect the observed frequency of potential sewage patterns at each site, based on the continuous data collected during baseflow characterization. At S2 and U4, target SPC conditions of 90 µS cm^{-1} and 180 µS cm^{-1}, respectively, occurred at a frequency of approximately one event in three days. At U3, target SPC conditions of 150 µS cm^{-1} occurred at a frequency of approximately one event per day.

Water samples were collected into acid-washed polypropylene bottles, returned to the laboratory on ice, then frozen until analysis. Samples were analyzed for nutrients and a suite of 25 ions and metals. Nutrients were analyzed at the University of Georgia Soil, Plant and Water Laboratory. Ions were analyzed at the University of Georgia Center for Applied Isotope Studies using ICP-OES. A subset of samples was also analyzed for *E. coli* by the Joye Research Group at the University of Georgia. These samples were collected into 710 mL Whirl-Pak bags (Nasco, Fort Atkinson, WI), returned to the laboratory on ice, and stored in a refrigerator for up to 24 hours until analysis. Water samples were analyzed for *E. coli* according to the US Environmental Protection Agency (EPA) Method 1603 for *E. coli* using modified mTec agar (BD, Franklin Lakes, New Jersey).

All water chemistry data from were analyzed by taking the mean and standard deviation of nutrients and major ions at each site. We then compared mean concentrations of analytes with baseflow samples taken during Sampling Period I to determine the relative increase or decrease that occurred during elevated SPC conditions. *E. coli* data were analyzed by taking the mean value at each site and comparing it to EPA water quality regulatory standards.

Hypothesis 3 - sediment

To test the hypothesis that sediment inputs were associated with changes in conductivity, we performed turbidity trials in the lab using clay soils, hereafter referred to as 'sediment', collected from the banks of Tanyard Creek. In each trial, sediment was added to 500 mL of tap water to reach predetermined threshold NTU values and continuously suspended using a magnetic stir plate and stir bar at a rate of 1000 rotations per minute (RPMs). In order to determine the value of SPC for identifying sediment pollution, we utilized regulatory standards from the Georgia Erosion and Sedimentation Act of 1975 (OCGA 12-7-6), which states that runoff of sediment from disturbed areas cannot exceed an increase of 25 NTU over baseline for waters supporting warm water fisheries. Trial 1 assessed the relationship between sediment and SPC below the 25 NTU regulatory threshold, while Trials 2 and 3 evaluated relationships in sediment conditions above the regulatory threshold (Table 2). Each trial lasted 30 minutes and consisted of SPC readings taken every 5 minutes, where sediment release commenced at minute 10 and continued in equal increments every 5 minutes through minute 25. Readings of SPC taken during all turbidity trials were plotted over time and compared to field data of hypothesized sediment inputs to test for similarity in patterns.

Table 1: Characterization of each site by stream name, GPS location (Latitude, Longitude), percent urbanization (% Urban), sampling duration, percent of forest cover (% Forest), percent of pasture cover (% Pasture) and drainage area in km^2. Sampling Period 1 refers to sites where data was collected from July 2015 to April 2016. Sampling Period 2 refers to sites where data was collected from October 2016 to January 2018.

Stream Name	*Site ID*	*Urbanization Category*	*Latitude*	*Longitude*	*Sampling Period 1*	*Sampling Period 2*	*% Urban*	*% Forest*	*% Pasture*	*Drainage Area (km^2)*
Bear Creek	R1	Rural	33.9674	-83.4973		X	5.53%	79.97%	8.23%	2.11
Tallassee Creek	R2	Rural	33.9766	-83.4846	X		18.41%	59.25%	19.06%	1.94
Shoal Creek	R3	Rural	33.9699	-83.3038	X	X	19.72%	24.69%	47.75%	2.10
Turkey Creek	S1	Suburban	33.9719	-83.4549	X	X	34.46%	45.32%	9.64%	10.14
Trail Creek	S2	Suburban	33.9549	-83.3647		X	41.10%	37.54%	14.25%	29.09
McNutt Creek	S3	Suburban	33.9262	-83.4629	X		41.93%	31.94%	15.19%	22.53
Carr Creek	U1	Urban	33.9370	-83.3525	X	X	62.94%	13.43%	2.74%	3.97
Brickyard Creek	U2	Urban	33.9743	-83.3957	X		75.35%	12.46%	5.40%	3.63
Brooklyn Creek	U3	Urban	33.9545	-83.3990	X	X	93.47%	4.86%	0.47%	0.96
Tanyard Creek	U4	Urban	33.9497	-83.3750		X	99.05%	0.85%	0.04%	2.13

Table 2: Target conditions for turbidity trials. All values are reported in Nephelometric Turbidity Units (NTU) where “Start NTU” is the turbidity conditions at the beginning of each trial, “Addition X” is the targeted total turbidity following the first, second, or third sediment addition, and “End NTU” is the final total turbidity desired for each trial.

	Start NTU	***Addition 1***	***Addition 2***	***Addition 3***	***End NTU***
Trial 1	5	10	15	20	25
Trial 2	5	15	25	35	45
Trial 3	5	30	55	80	105
Control	5	-	-	-	5

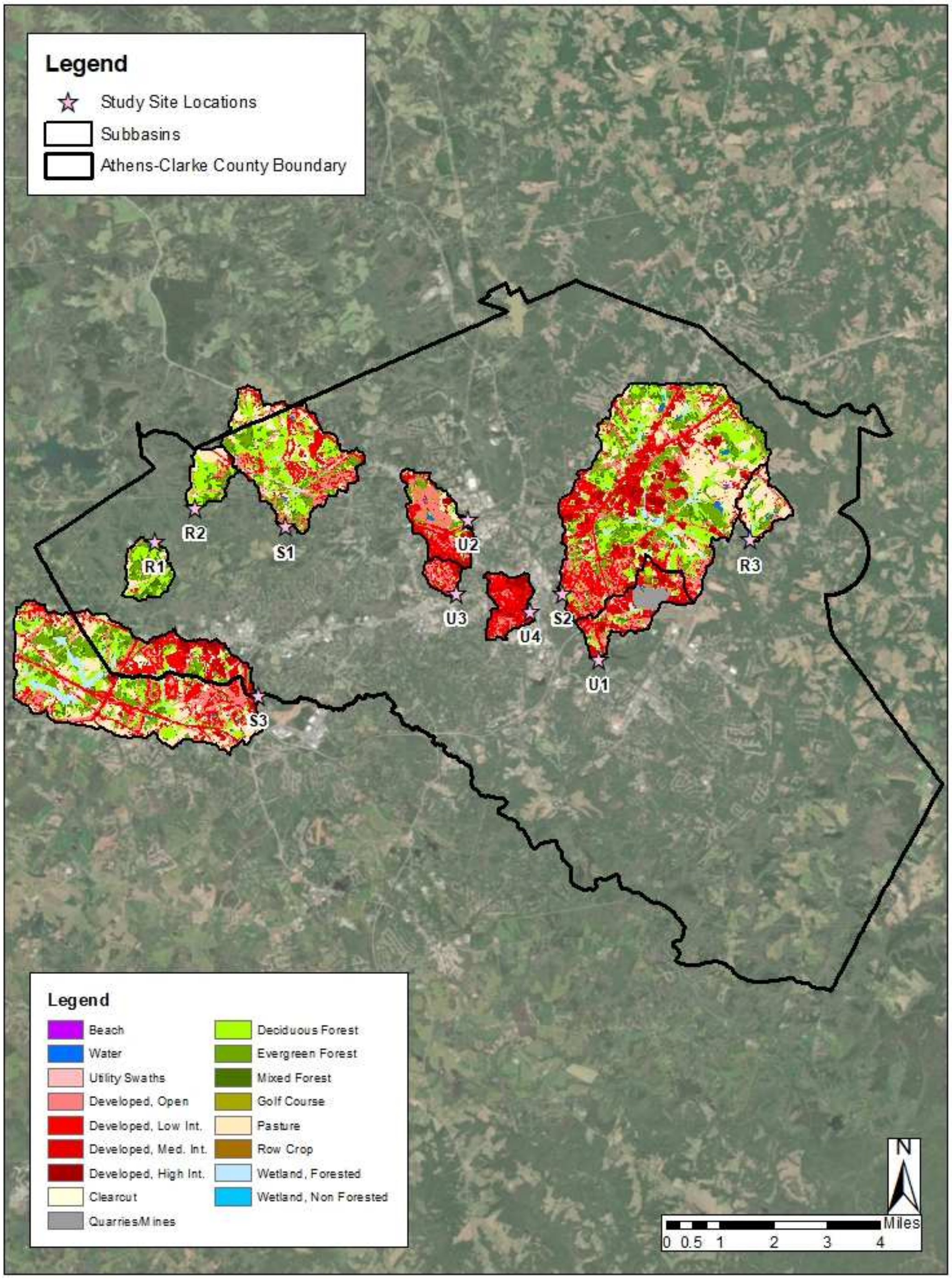

Figure 1: Map of all sampling sites and watershed land cover based on the 2008 Georgia Land Use Trends (GLUT 2008). Red colors represent developed land and green colors represent natural/forest cover.

CHAPTER 3

RESULTS

Sampling Period 1: Characterization of trends in SPC

Across all sites, mean temperature ranged from 15.4-26.9 ˚C, mean SPC ranged from 30.7-512 µS/cm, and mean stage height ranged from 0.24-0.61 m (Table 3). Temperature and stage height were variable across the urban gradient, while SPC was positively related to urbanization. Site R2 displayed the lowest mean SPC (30.7 µS/cm) while site U1 displayed the largest mean SPC (512 µS/cm).

Throughout the entire time series, SPC was highly variable within most sites except at R1, the most forested site, where it remained relatively constant over time (Figure 2). Normalized daily trends of SPC revealed that urban sites experienced a much larger range of SPC conditions within a single day than rural or urban sites (Figure 3). U2 and U3 displayed the largest daily variability in SPC across all sites with ranges of -0.5-0.10 µS/cm and -0.75-0.05 µS/cm, respectively. No consistent temporal pattern was observed in normalized daily trends of SPC, but in general, rural and urban sites peaked unimodally in the morning, then declined steadily until the evening when SPC began to rise again (Figure 3). Notably, sites U3 and U4 exhibited distinct deviations from this general trend. At U3, the daily trend displayed a large peak of SPC in the morning, followed by a smaller, second peak in the evening. At U4, the daily trend displayed a moderate peak of SPC in the morning, followed by a series of minor peaks and declines throughout the day.

A summary of baseflow water chemistry results is shown in Table 4. Water chemistry taken during baseflow showed that concentrations of NO_3, TN, DIN, PO_4, Cl, SO_4, Ca, K, Mg, and Na were positively correlated with urbanization and significantly elevated at the urban sites compared to the forested and suburban sites. Correlation analysis between all analytes at baseflow showed that SPC was strongly positively correlated with Mg, K, Ca, SO4 and Mn and moderately positively correlated with NO_3, NH_4, TN, Na, and Cl (Figure 4).

Sampling Period 2: Hypothesis testing

Hypothesis 1

CCF analysis revealed a negative temporal relationship between SPC and stage height at most of our sites. We interpreted this as dilution by rainwater: as stage height increased, we generally observed concurrent decreases in SPC. However, at two of our urban sites (U3 and U4) we saw brief positive relationships between SPC and stage height followed by negative correlations later in the time series, which we interpreted as a first flush. As these are the two sites with highest urban cover, we considered this as evidence in favor of Hypothesis 1 (Figure 5).

Closer analysis of SPC and stage height during precipitation events revealed that most sites experienced at least occasional elevated SPC at the initiation of stormflow, but the increases were more consistent and pronounced at urban sites compared to rural and suburban sites. When summarized across urbanization categories, the elevation of SPC during stormflows was greatest at urban sites (11.2 μS/cm) and lowest at rural sites (2.6 μS/cm). U4 displayed the greatest change in SPC at 31.5 μS/cm, which was 52.5x greater than R2, which displayed the lowest change in SPC at 0.6 μS/cm (Table 5). We interpreted these results as additional support for Hypothesis 1.

Hypothesis 2

Water chemistry samples taken at sites U3 and U4 during peak SPC conditions revealed that most, but not all, analyte concentrations were elevated when compared with baseflow water chemistry at the same site (ratio > 1.0) (Table 6). At U3, concentrations of NH_4 were nearly 9x higher during peak SPC conditions. However, concentrations of NO_3 and TN were not similarly elevated. Concentrations of Si and TP decreased slightly during elevated SPC conditions. At U4, concentrations of Mg, Mn, Na, NH_4, and TP were nearly 1.5x higher than at baseflow.

Manganese showed large increases in concentrations at both sites. *E. coli* concentrations at all three sites were 1.6-4.5x higher than the EPA water quality standard of 200 CFU/100mL for the months of May through October (Table 6). However, we lacked baseflow *E. coli* concentrations for comparison. Correlation analysis between nutrients and ions showed that SPC was strongly positively correlated with Mg and TN (Figure 6). Water chemistry analyses for samples taken during peak SPC conditions which did not occur coincidently with peak stage height conditions showed some support for Hypothesis 2, that sewer leaks may be revealed by changes in SPC which occur in regular, non-random patterns independent of changes in stage height.

Hypothesis 3

Patterns of SPC recorded during turbidity trials showed that SPC readings during sediment release were not significantly higher or more variable compared to SPC immediately prior to release of sediment. The largest variation occurred during Trial 3, where SPC increased by 9 μS/cm, reaching a maximum SPC of 142 μS/cm. Mean SPC was slightly elevated for trial durations but did not differ significantly from the control (Table 9). These results do not support Hypothesis 3, that random and irregular fluctuations in SPC are indicative of sediment inputs from riparian areas.

Table 3: Summary of in-stream conditions at each site. Readings for specific conductivity (μS cm^{-1}), stage height (meters), and temperature (degrees Celsius) were taken every 5 minutes using in-situ data loggers. Mean (standard deviation), minimum (Min), and maximum (Max) recorded values were summarized over the total sampling duration at each site. Sampling periods for each site are outlined in Table 1. Data was cleaned prior to analysis by excluding known logger errors, including erroneous measurements, improper installation of loggers, and periods of logger inactivity.

	Stage Height (m)			***Specific conductivity (μS cm^{-1})***			***Temperature (˚C)***		
	Mean	*Min*	*Max*	*Mean*	*Min*	*Max*	*Mean*	*Min*	*Max*
R1	0.3 (0.14)	0.05	0.73	53.8 (11.5)	17.2	140.8	15.4 (4.3)	4.8	24.3
R2	0.24 (0.06)	0.11	0.28	30.7 (7.3)	2.1	113.2	16.9 (4.6)	6.8	25.3
R3	0.41 (0.23)	0.07	1.05	61.8 (13)	6.3	526.7	20.6 (12.7)	4.8	21.2
S1	0.49 (0.35)	0.02	1.6	65.4 (9.8)	3.3	210.2	20.8 (16.1)	4.2	26.8
S2	0.5 (0.35)	0.04	1.49	79.3 (12.4)	18.7	133	17.5 (5.8)	4.2	29.2
S3	0.48 (0.14)	0.21	0.42	57.2 (9.2)	2.5	368.1	17.2 (5.6)	-2.5	27.2
U1	0.61 (0.34)	0.08	1.34	512 (100.9)	28	933.2	24.5 (16.9)	5.7	24.1
U2	0.35 (0.08)	0.23	0.56	137.2 (24.7)	25.2	252.4	17.6 (5.4)	6.2	29.9
U3	0.41 (0.23)	0.04	0.99	79.1 (21.5)	5.7	1044.2	24.5 (17.3)	5.8	24.8
U4	0.38 (0.26)	0.01	2.4	177.1 (35.5)	15.5	1092.7	26.9 (17.2)	7.4	22.6

Table 4: Mean (standard deviation) of water chemistry data collected during Sampling Period 1. SPC data were collected continuously at 5-minute intervals while water chemistry samples were collected in June and October 2015 at all sites except S2, which does not have data for this sampling period. S2 was added to the study during Sampling Period 2 to reflect management priorities, as stated by the Athens-Clarke County Transportation and Public Works Department (ACC TPWD). Units are reported in mg L^{-1} unless otherwise noted. Sites are listed left-to-right in order of increasing percent imperviousness as defined in Table 1. The number of water chemistry samples analyzed equals two in all cases except for site R1 analyte PO4, which is represented by a single data point due to suspected contamination during analysis of the October 2015 sample.

	R1	***R2***	***R3***	***S1***	***S2***	***S3***	***U1***	***U2***	***U3***	***U4***
SPC (µS cm^{-1})	49.05 (1.34)	32.25 (1.06)	58.91 (0.12)	59.00 (11.31)	--	61.00 (4.24)	576.80 (19.52)	146.50 (7.78)	84.10 (18.24)	189.70 (3.82)
NO_3	0.13 (0.09)	0.23 (0.02)	1.31 (0.51)	0.34 (0.03)	--	0.39 (0.02)	4.74 (1.34)	1.19 (0.52)	1.15 (0.10)	2.44 (0.00)
NH_4 (µg L^{-1})	14.03 (2.86)	32.55 (13.60)	19.88 (9.57)	22.30 (8.00)	--	36.40 (3.86)	156.49 (174.20)	31.31 (8.36)	105.80 (102.56)	42.59 (16.04)
TN	0.30 (0.06)	0.46 (0.12)	1.99 (0.38)	0.60 (0.14)	--	0.63 (0.03)	5.41 (1.24)	1.82 (0.02)	1.36 (0.03)	2.77 (0.13)
DIN (µg L^{-1})	141.52 (89.84)	265.55 (34.82)	1334.38 (520.82)	363.30 (24.54)	--	424.90 (22.95)	4896.48 (1165.06)	1222.31 (514.90)	1252.30 (7.10)	2480.08 (12.50)
PO_4 (µg L^{-1})	10.71*	4.64 (1.75)	7.03 (1.12)	6.96 (3.30)	--	5.38 (0.69)	4.65 (1.22)	16.51 (9.80)	33.10 (29.76)	27.85 (19.06)
TP (µg L^{-1})	17.18 (6.14)	14.76 (4.48)	37.31 (4.45)	19.14 (6.80)	--	19.09 (4.13)	16.14 (6.14)	64.40 (47.90)	34.23 (19.14)	36.95 (27.54)
Cl	2.86 (2.14)	1.99 (0.37)	4.30 (0.14)	2.97 (0.17)	--	3.82 (0.57)	13.32 (0.23)	7.62 (0.40)	10.56 (4.58)	19.45 (5.33)
SO_4	1.27 (0.23)	0.74 (0.45)	1.43 (0.70)	1.17 (0.52)	--	2.97 (2.14)	198.57 (40.21)	9.80 (10.92)	10.11 (2.26)	18.67 (3.05)
HCO_3	4.54 (0.51)	2.14 (0.34)	3.04 (0.48)	5.29 (1.11)	--	3.88 (0.54)	2.07 (0.61)	6.15 (3.05)	6.02 (3.99)	5.69 (1.54)
CO_3	0.00 (0.00)	0.00 (0.00)	0.00 (0.00)	0.01 (0.01)	--	0.00 (0.01)	0.00 (0.00)	0.00 (0.00)	0.00 (0.00)	0.00 (0.01)
Ca	3.40 (0.51)	1.51 (0.46)	3.78 (0.57)	4.50 (0.41)	--	4.08 (0.86)	62.74 (7.67)	13.41 (2.83)	4.89 (0.64)	14.02 (0.98)
K	1.81 (0.04)	1.10 (0.08)	2.45 (0.46)	1.63 (0.45)	--	1.78 (0.30)	8.20 (0.61)	3.00 (0.05)	2.07 (0.07)	3.00 (0.58)
Mg	1.49 (0.10)	0.94 (0.20)	1.30 (0.10)	1.68 (0.06)	--	1.31 (0.11)	10.95 (0.62)	3.13 (0.01)	1.26 (0.10)	2.99 (0.50)
Mn	0.03 (0.01)	0.03 (0.01)	0.02 (0.02)	0.06 (0.02)	--	0.09 (0.03)	0.96 (0.02)	0.03 (0.01)	0.01 (0.00)	0.02 (0.01)
Na	3.21 (0.12)	2.03 (0.43)	3.59 (0.05)	4.08 (0.26)	--	3.40 (0.22)	8.73 (0.49)	5.87 (0.82)	5.75 (1.50)	9.94 (0.09)
Si	13.49 (12.92)	7.09 (7.58)	8.86 (9.58)	16.18 (8.14)	--	9.42 (6.46)	6.66 (7.87)	16.28 (1.07)	8.10 (6.01)	14.15 (1.45)
Sr	0.03 (0.00)	0.01 (0.01)	0.04 (0.00)	0.03 (0.00)	--	0.03 (0.00)	0.16 (0.02)	0.08 (0.01)	0.04 (0.00)	0.10 (0.00)
Zn	0.00 (0.00)	0.00 (0.00)	0.00 (0.00)	0.00 (0.00)	--	0.00 (0.00)	0.06 (0.08)	0.00 (0.00)	0.00 (0.00)	0.00 (0.00)

Table 5: Minimum, maximum, and mean of stormflow SPC aggregated by imperviousness and site for all identified storm events. Stormflow SPC was determined by identifying the SPC value recorded 20 minutes prior to the start of a precipitation event. The change in SPC from baseflow during storm events (ΔSPC) was calculated by subtracting the mean SPC value for stormflows from the mean SPC value during baseflow prior to storm events. The sampling period for each site is outlined in Table 1. The number of storm events assessed varies by site and ranges from 85-284 events. In all cases, ΔSPC is positive, which represents an increase in SPC during stormflows, and the largest ΔSPC values occur at the more urbanized sites. All values are reported in μS cm^{-1}.

	***Min* (*μS cm^{-1}*)**	***Max* (*μS cm^{-1}*)**	***Storm Mean* (*μS cm^{-1}*)**	***Pre-Storm Mean* (*μS cm^{-1}*)**	***ΔSPC* (*μS cm^{-1}*)**
summarized by site					
R1	35.5	140.8	58.6	56.1	2.5
R2	18.6	113.2	32.0	31.3	0.6
R3	34.7	274.3	64.9	61.3	3.6
S1	42.6	210.2	68.6	66.0	2.6
S2	55.0	124.6	82.1	79.2	3.0
S3	103.9	252.4	149.0	144.0	5.0
U1	212.0	933.2	518.2	516.9	1.3
U2	103.9	252.4	149.0	144.0	5.0
U3	46.9	1044.2	106.4	92.2	14.2
U4	92.0	1092.7	221.5	190.0	31.5
summarized by ISC category					
Rural	18.6	274.3	54.3	51.7	2.6
Suburban	42.6	252.4	96.4	93.0	3.4
Urban	46.9	1092.7	263.2	251.9	11.2

Table 6: Summary of water chemistry data collected from January to August of 2018. Sampling occurred at sites S2, U3, and U4 where real time remote monitoring stations were installed. Samples were automatically collected during high SPC conditions at real-time remote monitoring stations. We calculated mean (standard deviation) of nutrient and ion concentrations at each site, then determined the ratio of mean ionic concentrations at peak SPC conditions compared to mean ionic concentrations at baseflow SPC conditions. Ratio values greater than 1 indicate higher concentrations at peak SPC conditions, while values less than 1 indicate higher concentrations at baseflow SPC conditions. For example, peak calcium (Ca) concentration was 1.21x higher than baseflow concentrations at U3 but was 0.83x lower than baseflow concentrations at U4.

	S2 Peak Mean	***U3 Peak Mean***	***U3 Ratio***	***U4 Peak Mean***	***U4 Ratio***
SPC (µS cm^{-1})	87.33 (0.47)	158.17 (11.19)	1.881	655.50 (447.50)	3.455
Ca	2.19 (0.27)	6.40 (1.09)	1.21	6.80 (0.12)	0.83
K	1.45 (0.17)	3.19 (1.02)	1.33	2.36 (0.30)	1.48
Mg	0.58 (0.10)	1.66 (0.28)	1.15	1.86 (0.46)	1.54
Mn	0.03 (0.01)	0.05 (0.07)	2.66	0.02 (0.00)	1.74
Na	2.24 (0.20)	5.45 (0.51)	1.04	5.42 (0.77)	1.62
NH4	0.03 (0.03)	0.10 (0.20)	8.88	0.00 (0.00)	1.38
NO3	0.66 (0.12)	1.07 (0.16)	1.1	2.82 (0.18)	1.12
PO4	0.01 (0.00)	0.01 (0.00)	1.26	0.03 (0.03)	1.06
Si	5.14 (0.36)	9.28 (3.95)	0.76	4.15 (2.28)	0.48
Sr	0.02 (0.00)	0.04 (0.00)	1.03	0.05 (0.00)	1.13
TN	4.29 (0.41)	4.74 (0.86)	1.02	6.31 (0.34)	1.42
TP	0.06 (0.00)	0.08 (0.02)	0.95	0.08 (0.04)	1.55
E. coli (CFU)	2132	899.67	--	325	--

Table 7: Readings of SPC taken at the start, end, and every 5 minutes during turbidity trials.

Conditions for each trial are listed in Table 2.

	SPC (µS cm-1)			
	Control	***Trial 1***	***Trial 2***	***Trial 3***
Start	134	133	135	133
5 min	133	134	137	137
10 min	134	135	135	137
15 min	134	134	136	141
20 min	134	134	136	140
25 min	134	134	137	142
End	134	135	137	141

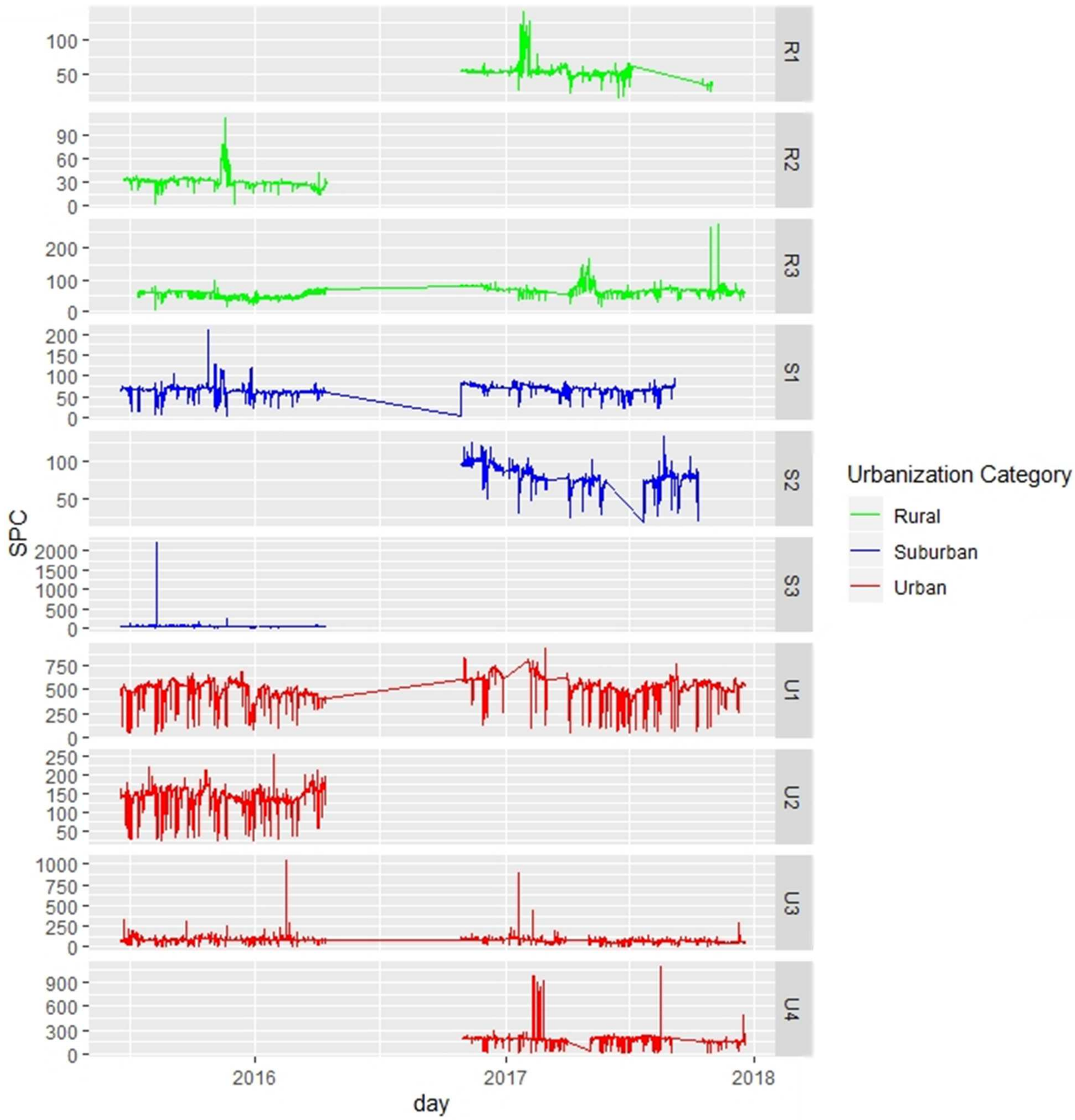

Figure 2: Complete time series of SPC readings taken at each of the 10 sites. Line colors correspond to classification of sites based on urbanization categories. Green represents rural sites, blue represents suburban sites, and red represents urban sites.

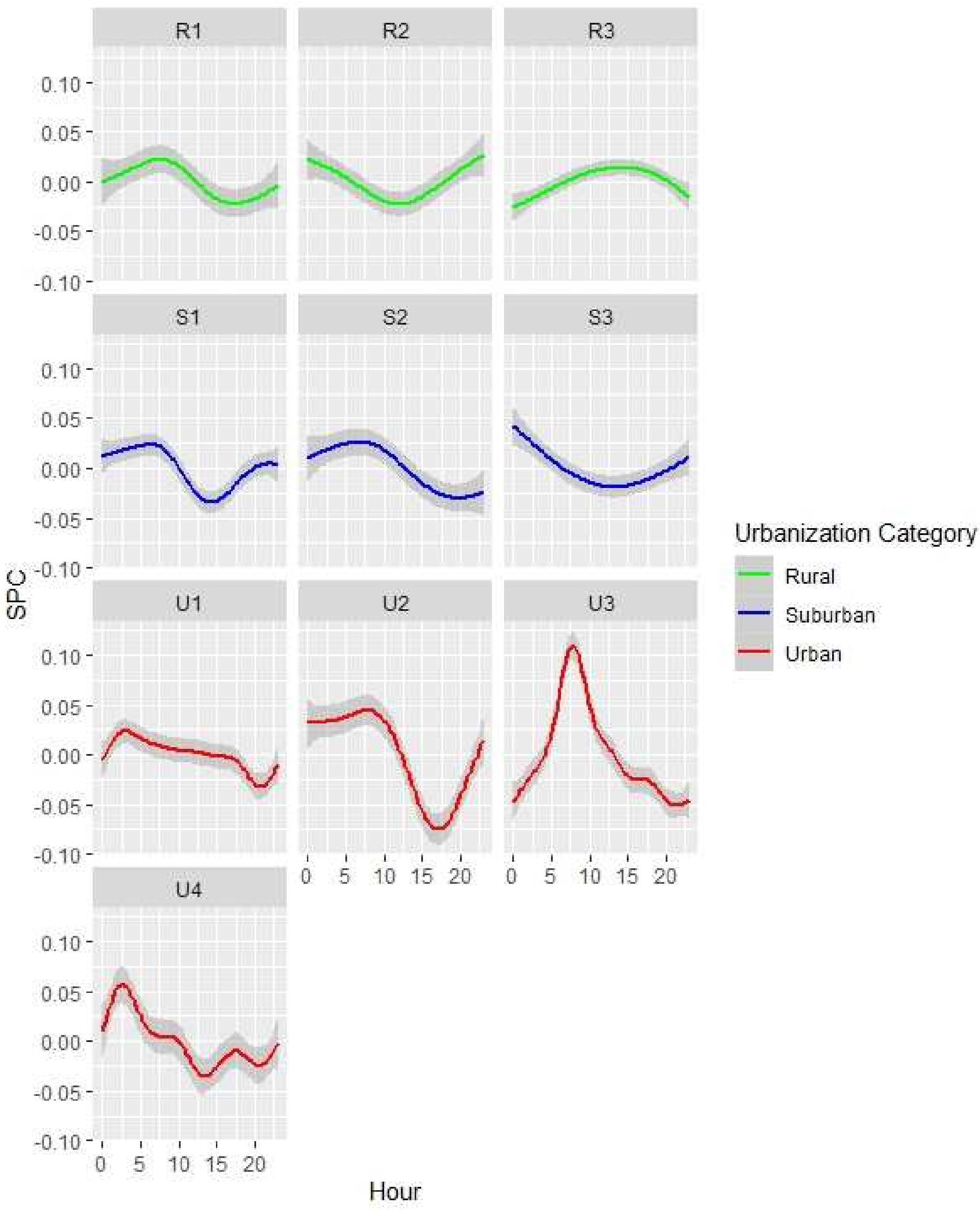

Figure 3: Normalized daily trends of SPC based on continuous data collected at five-minute intervals at each site. Variation from the mean value is on the y-axis and time of day is on the x-axis on a 24-hour time scale from 12:00AM to 11:59PM.

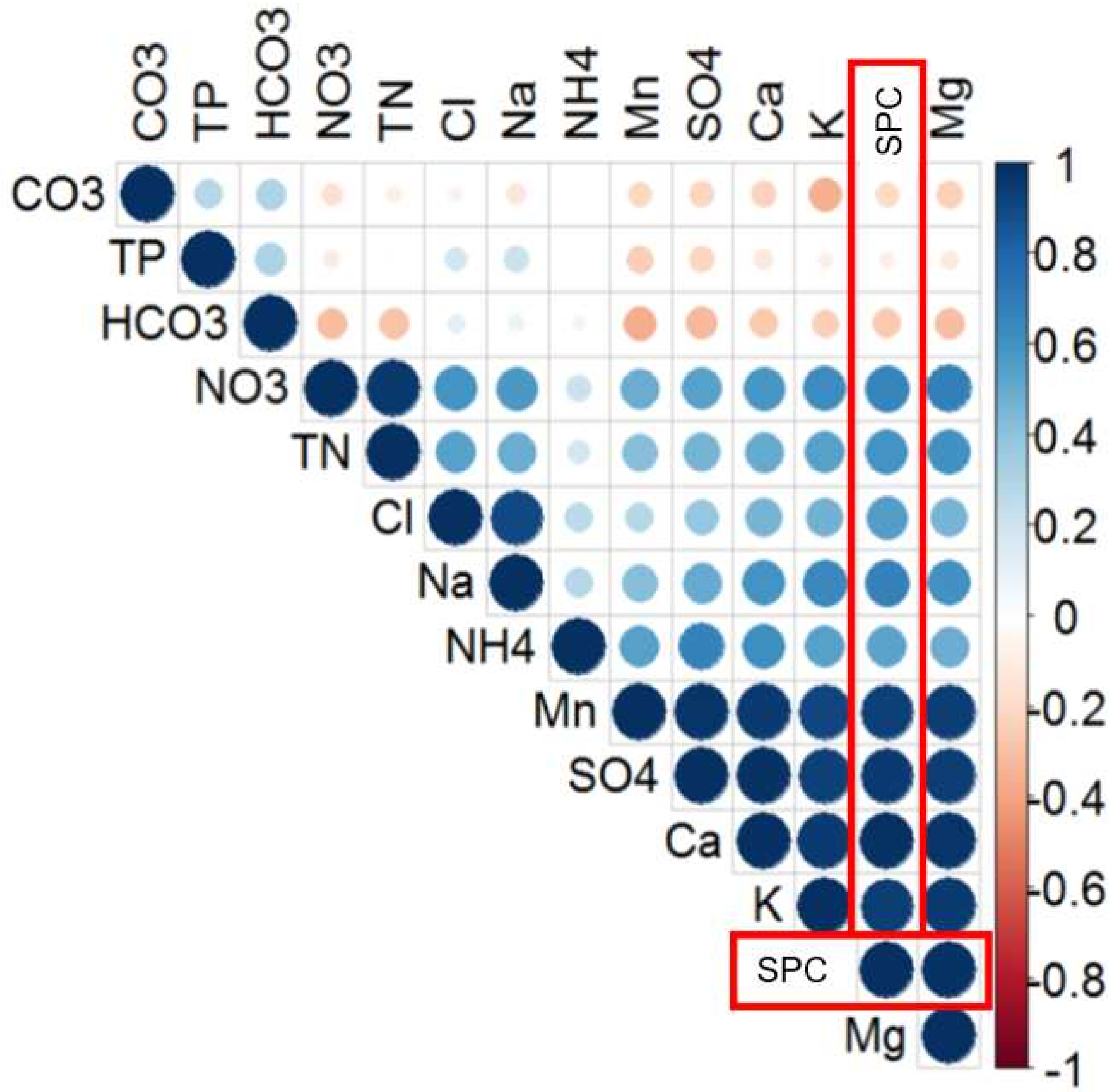

Figure 4: Heat map of correlation between nutrients and ions across all baseflow water chemistry samples at all sampled sites. Two baseflow water chemistry samples were collected at each site during Sampling Period 1 (Table 1), where the first and second samples were collected in June and October 2015, respectively. The size of each dot represents the strength of the correlation between the two intersecting analytes, while the color represents the positive (blue) or negative (red) direction of the relationship.

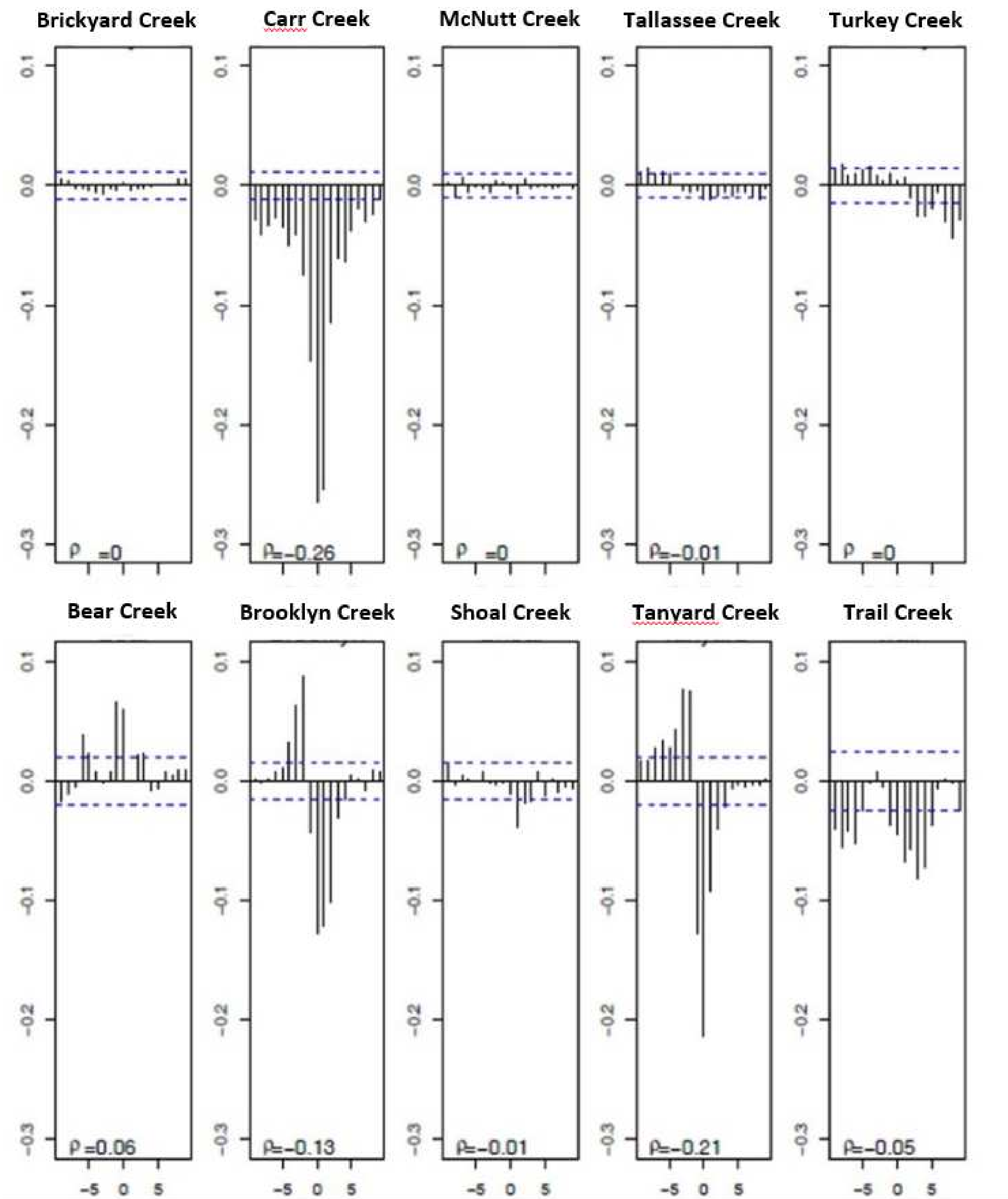

Figure 5: Cross correlation of SPC and stage height at each site. The y-axis represents the strength and direction of the relationship between SPC and stage height, while the x-axis represents the number of time lags (k), where a single time lag equals 10 minutes.

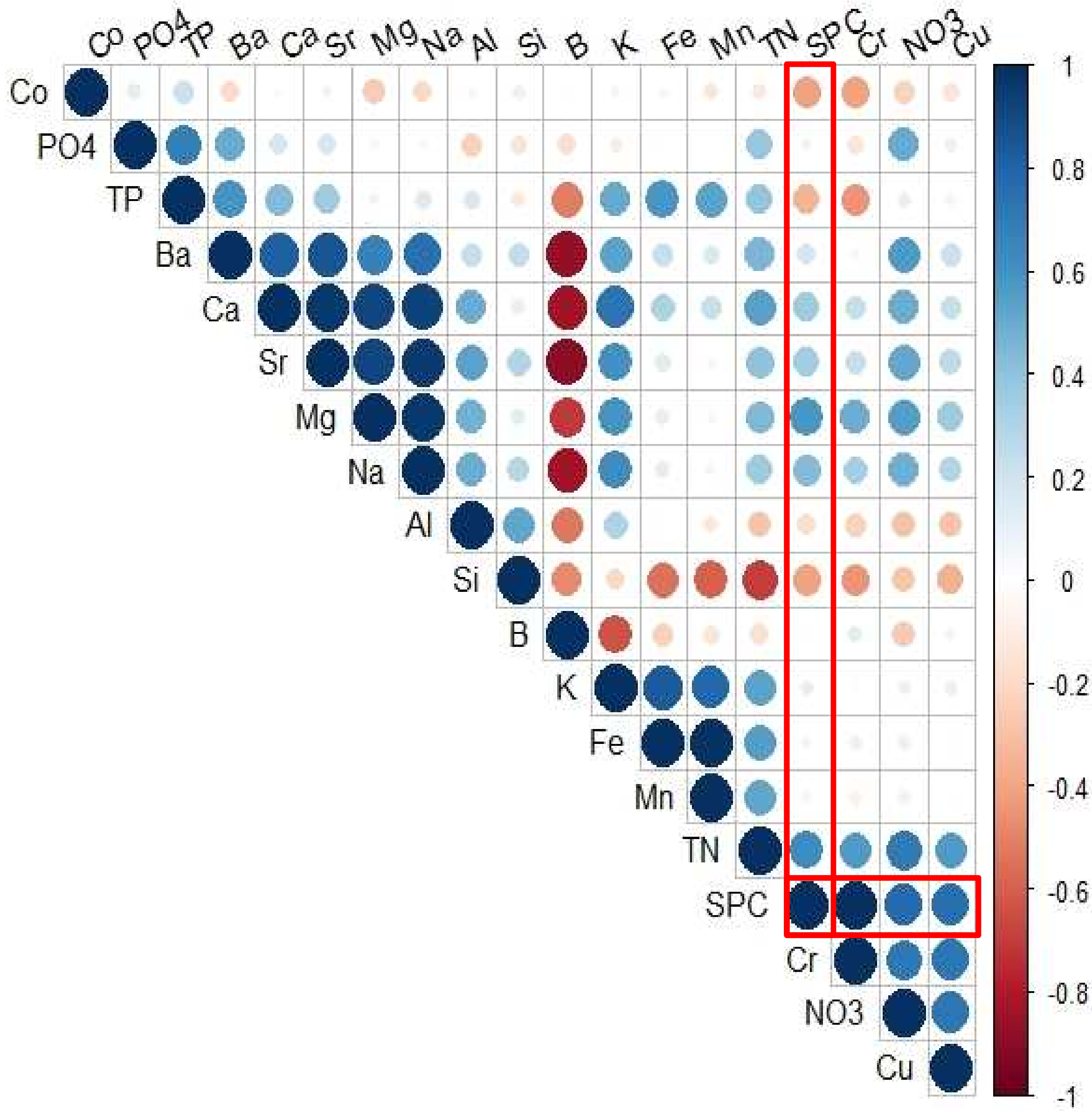

Figure 6: Heat map of correlation between nutrients and ions across all samples collected at sites S2, U3 and U4 using automated water chemistry sampling. Samples were collected from January to August 2018. The size of each dot represents the strength of the correlation between the two analytes, while the color represents the positive (blue) or negative (red) direction of the relationship.

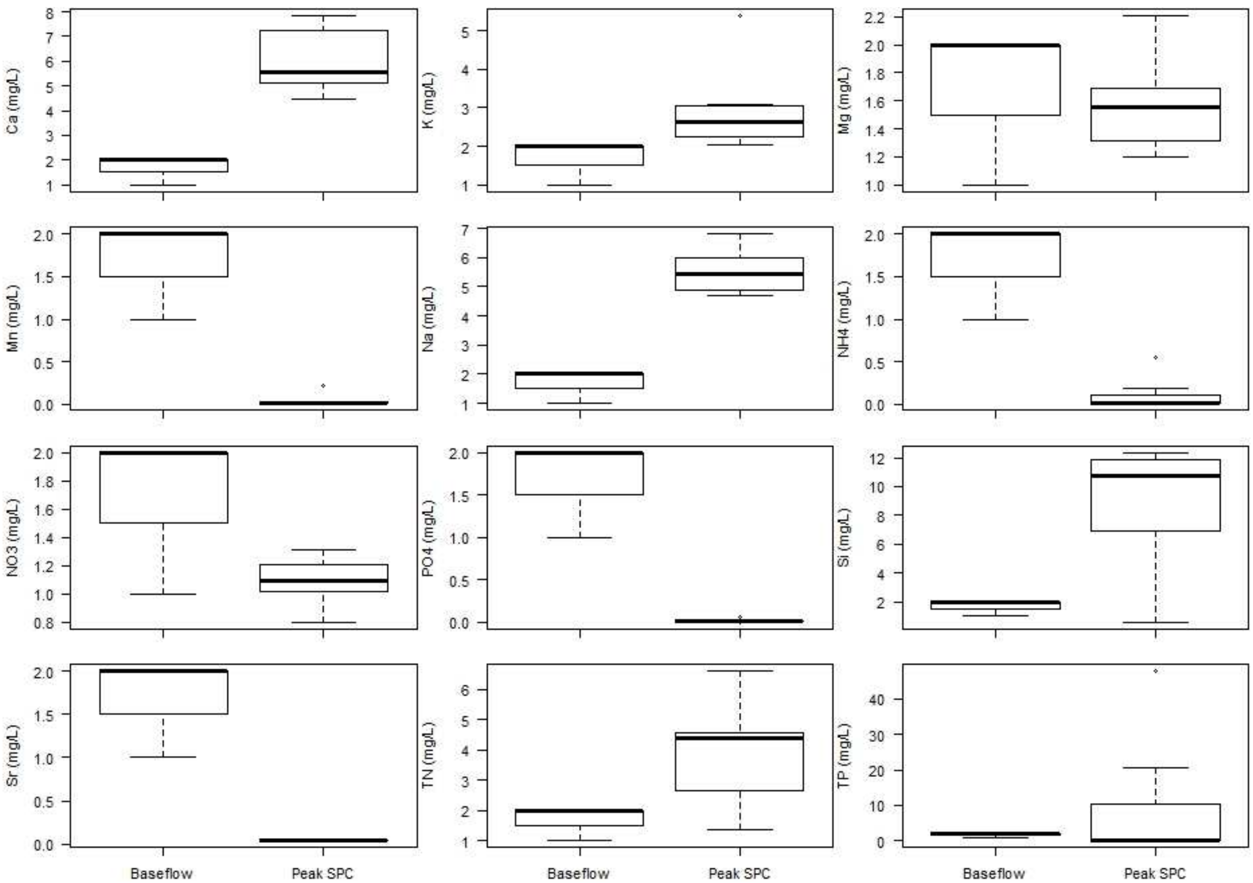

Figure 7: Boxplot of ionic concentrations at site U3 comparing water chemistry of samples taken at baseflow to that of samples taken during peak SPC conditions. Concentration of analytes is represented on the y-axis where the scale on each plot is adjusted to encompass the range of variability for each analyte. Boxes represent the median and first and third quartiles while whiskers represent the minimum and maximum.

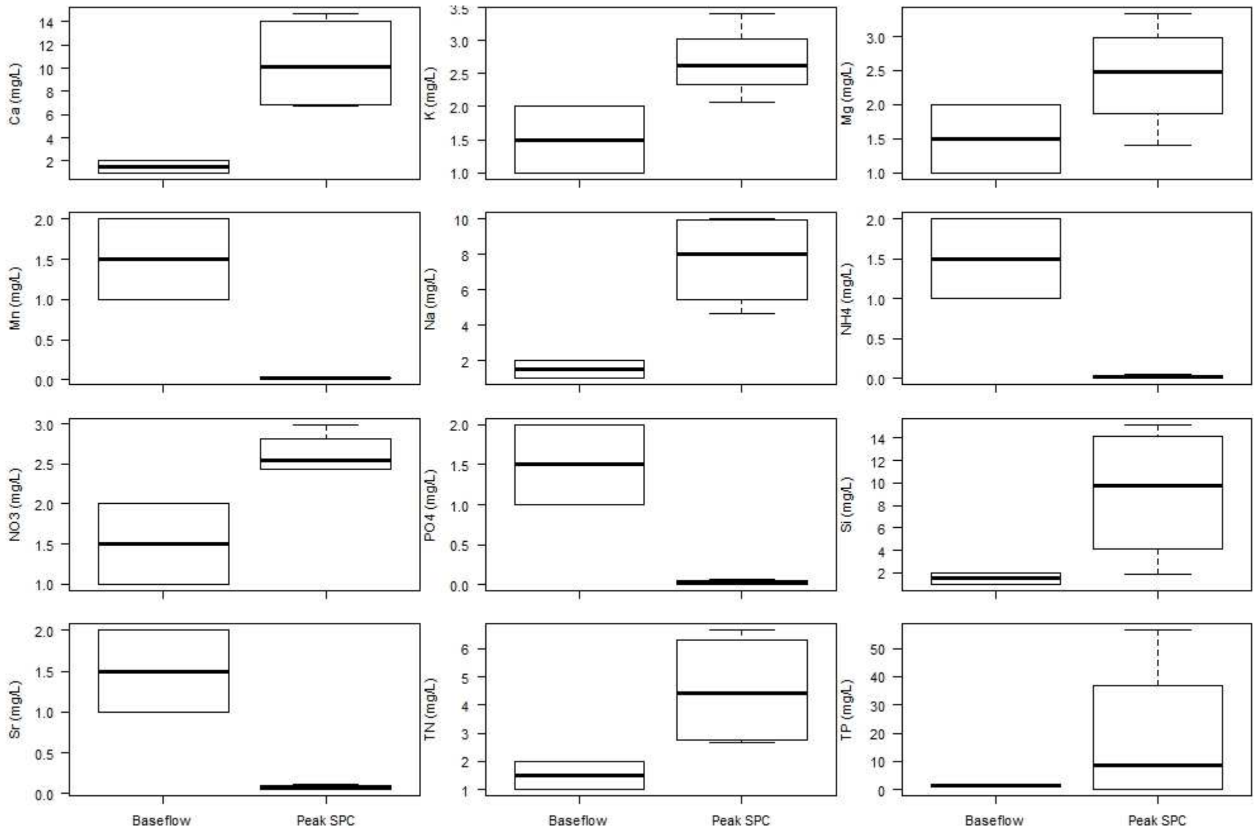

Figure 8: Boxplot of ionic concentrations at site U4 comparing water chemistry of samples taken at baseflow to that of samples taken during peak SPC conditions. Concentration of analytes is represented on the y-axis, where the scale on each plot is adjusted to encompass the range of variability for each analyte. Boxes represent the median and first and third quartiles while whiskers represent the minimum and maximum.

CHAPTER 4

DISCUSSION

Conductivity as a monitoring metric

A growing body of work indicates the need for management tools that address multiple water quality stressors simultaneously, rather than single contaminants (Kaushal et al., 2018). In particular, the emerging “freshwater salinization syndrome” (Kaushal et al., 2018; Kaushal et al., 2019) proposes that concurrent trends in SPC, pH, alkalinity, and base cations are indicative of a human-induced shift in freshwater chemical composition and processes in North America. This shifting chemical composition hinders many ecosystem services provided by freshwater systems and leads to negative impacts on human resources and human and biotic health. Elevated salinization has been strongly correlated with degraded stream macroinvertebrate community health and can lead to acute toxicity in some species, withimplications for overall biotic integrity in freshwater systems (Horrigan et al., 2004; Horrigan et al., 2007; Kaushal et al., 2017). SPC is a useful indicator of the freshwater salinization syndrome because it is often used as a proxy measurement for salinity. In addition, SPC is a strong indicator of a variety of stressors associated with urban watershed disturbance, including inputs from sewage, sediment, road salting, and transportation infrastructure (Anderson et al. 2004, Daley et al. 2009, Kaushal et al. 2018). With advances in sensor technology, the capacity to collect high resolution spatial and temporal data is becoming increasingly accessible and provides an opportunity for the expanded use of SPC as a management tool.

In this study, continuous monitoring of SPC in streams across a gradient of urbanization revealed fine-scale temporal variability in SPC that is likely indicative of multiple distinct urban pollutants. Evaluation of patterns in SPC resulted in support for Hypothesis 1, the detection of the stormwater first flush effect, partial support for Hypothesis 2, the detection of sewage inputs, and no support for Hypothesis 3, the detection of sediment inputs. Despite these mixed results, we conclude that there is sufficient evidence to promote continuous monitoring of SPC as a useful tool for detecting episodic water quality impacts to urban streams from multiple stressors. When paired with real-time monitoring technology, these results establish a baseline for the application of continuous SPC data as an indicator of and first-warning system for specific pollution events, such as illicit discharges, stormwater runoff and sewage leaks.

This study provided evidence for the use of SPC as an indicator of the first flush effect. When assessed across a gradient of urbanization, CCF of SPC with stage height showed that our two most urban sites, U3 and U4, displayed brief positive relationships between SPC and stage height followed by sustained negative correlations, while all other sites showed consistent negative relationships between SPC and stage height. Stormflow peak SPC values displayed greater changes from baseflow SPC values at urban sites compared to rural and suburban sites, supporting the use of continuous conductivity monitoring for detection of the FFE.

When used in conjunction with real-time monitoring systems, SPC has potential to serve as a single, simple metric for rapid detection of disturbance associated with stormwater runoff. For local governments, management of stormwater runoff often requires a significant amount of both time and resources, because monitoring of stormwater quality is mandated by the Federal Clean Water Act (CWA) (33 U.S.C. §§1251-1387). Real time monitoring of SPC could be applied in several ways to enhance regulatory compliance under the CWA. If applied strategically throughout watersheds to in proximity to permitted discharges, continuous monitoring of SPC could allow managers to monitor compliance with stormwater discharge permits at industrial facilities. In addition to regulatory requirements, it is also in a municipality's interest to effectively transport and discharge of stormwater from public property, such as parks, roadways, and sidewalks, because of the physical damage that stormwater can cause to infrastructure. If applied at fine-scale spatial resolutions, continuous monitoring of SPC could assist in assessing the performance of stormwater infrastructure, both traditional and 'green', for detaining and treating runoff.

Water chemistry revealed that baseflow concentrations of nearly all major ions were elevated at urban sites compared to rural or suburban sites. Sulfate, calcium, potassium, and manganese were strongly positively correlated with SPC across all sites, which suggests that baseflow SPC in Athens-Clarke County streams is driven by a combination of geologic and urban factors. While calcium is usually associated with mineral weathering (Drever 1997; Rose 2002; Griffith 2014), elevated sulfate and potassium has been associated with urbanization in Georgia Piedmont streams (Rose 2002; Rose 2007). Peak SPC water chemistry showed strong positive correlations of SPC with chromium, total nitrogen, nitrate, and copper. Elevated concentrations of chromium and copper are considered a common feature of urban streams (Paul & Meyer 2001). Sources of chromium and copper in urban watersheds include brake linings, tires, and metal alloys which accumulate on roads and parking lots and are carried into streams by stormwater runoff. Elevated concentrations of nitrate and other nitrogen compounds have been recorded downstream of urban centers which receive direct inputs of untreated sewage effluent. In addition, other studies from around the world have noted diel patterns in SPC and ionic concentrations which correlated with human activity in the watershed, such as decreased concentrations at night (low human activity) and elevated concentrations during daytime (high human activity; Santos et al., 2019). Time series plots of SPC show that continuous monitoring at a 5-minute time scale is sensitive enough to change rapidly in response to natural and human inputs. Normalized daily trends of SPC recorded during this study suggest that urban sites display greater variability in SPC than non-urban sites, with higher daytime peaks and lower nighttime lows. These results may indicate support for Hypothesis 2, which asserted that regular, nonrandom patterns in SPC are indicative of sewage inputs. However, this should be verified with monitoring of fecal coliform and other more direct indicators of sewer leaks.

Sediment addition experiments did not reveal relationships between SPC and inputs of surface sediment from surrounding soils, such as might be observed downstream of cleared land due to development and other urban activity. While there are clear relationships between surrounding geology and SPC (Drever 1997, Griffith 2014), soils in the Piedmont contain relatively low ionic concentrations compared to other regions in the USA. It is possible that in physiographic regions with soils with high ionic concentrations, continuous monitoring of conductivity could prove to be a useful indicator of erosion events.

Limitations of continuous monitoring techniques

In this study we explored two methods for collecting continuous water quality data using remote sensing technology. Continuous monitoring using “disconnected” in-situ devices, such as the HOBO loggers used in this study, requires very little knowledge of software or programming and provides straightforward installation and data retrieval. However, data cannot be accessed in real-time, and instrument costs are much higher than DIY systems. Lack of real-time reporting also means that errors take longer to detect. Over the course of this study, several months of data were rendered unusable due to logger errors, such as loggers being buried under sediment or installed improperly, that were not discovered until after data collection had ended. Real-time monitoring technologies provide more reliable data collection due to the ability to monitor systems and identify errors immediately. However, these DIY systems require significant knowledge of software and programming in order to assemble and operate the technology. Installation of these systems also requires more space, time, and materials due to the need for external power sources such as solar panels and large batteries. While HOBO loggers can be installed readily in a variety of locations, real-time monitoring stations must be anchored to streambanks within close range of solar panels so that appropriate power connections can be maintained. Despite this, real-time technologies are becoming simpler and more user friendly as these systems becomes more widely used and promoted through programs like the Stroud Water Research Center’s EnviroDIY (https://www.envirodiy.org/). Both forms of remote sensing also produce a large amount of data, which can be cumbersome to manage and manipulate for analysis.

Use of SPC as a monitoring metric would be complemented by the collection of additional water quality data, such as concurrent water chemistry and microbial sampling. In this study, we were limited in our ability to collect a large number of contemporaneous water chemistry and *E. coli* samples due to the time required to develop each real-time monitoring station. The small sample size did not allow us to compare directly between high SPC conditions at each real-time monitoring site and monitoring of conductivity alone cannot provide direct evidence of specific pollutants. In addition, sediment experiments were fairly limited in their scope and turbidity was not measured in-situ during this study. Real-time monitoring technology for turbidity is available and compatible with systems used in this study. Experiments performed in this study to test for Hypothesis 3 may have been enhanced through a better understanding of temporal and spatial variability in turbidity.

Future considerations

Despite the drawbacks outlined above, this study demonstrates the many advantages to the use of real-time systems for monitoring of water quality. The customizability of real-time technology provides endless potential for monitoring programs, and the relatively inexpensive technology could be deployed broadly at a fine spatial scale to provide highly detailed insights into stressors. In addition, these systems are portable enough to be redeployed multiple times as monitoring priorities shift with continuous management. With the right programming knowledge, managers can tailor monitoring stations to meet very specific local needs and personal preferences. Real-time systems can easily be coupled with notification systems, such as email or text alerts, which notify managers of concerning water quality conditions and lead to more targeted sampling programs. If deployed downstream of stormwater control structures throughout a watershed, real-time monitoring of SPC could provide instantaneous feedback on performance and efficacy of stormwater infrastructure, helping managers to track and report the functional status of stormwater infrastructure.

REFERENCES

Ancona, M., N. Corradi, A. Dellacasa, G. Delzanno, J.-L. Dugelay, B. Federici, P. Gourbesville, G. Guerrini, A. La Camera, P. Rosso, J. Stephens, A. Tacchella, G. Zolezzi. 2014. On the design of an intelligent sensor network for flash flood monitoring, diagnosis, and management in urban areas. Procedia Computer Science 32:941-946.

Anderson, c., G. Lewis, K. Sargent, D. Sarkar. 2004. Influence of wastewater treatment effluent on concentrations and fluxes of solutes in the Blush River, South Carolina, during extreme drought conditions. Environmental Geosciences 11(1):28-41.

Baker, M.E., M.L. Schley, J.O. Sexton. 2019. Impacts of expanding impervious surface on specific conductance in urbanizing streams. Water Resources Research, SS, 6482-6498.

Booth, D.B., A.H. Roy, B. Smith, K.A. Capps. 2016. Global perspectives on the urban stream syndrome. Freshwater Science 35(1):412-420.

Cohen, B. 2006. Urbanizaiton in developing countries: current trends, future projections, and key challenges for sustainability. Technology in Society 28:63-80.

Daley, M., J. Potter, W. McDowell. 2009. Salinization of urbanizing New Hampshire streams and groundwater: effects of road salt and hydrologic variability. Journal of the North American Benthological Society 28(4):929-940.

Deletic, A. 1998. The first flush load of urban surface runoff. Water Research 32(8):2462-2470.

Drever, J.I. 1997. The geochemistry of natural waters, 3rd edn. Prentice Hall, Upper Saddle River, NJ.

Eidsen, G.W., S.T. Esswein, J.B. Gemmill, J.O. Hallstrom, T.R. Howard, J.K. Lawrence, C.J. Post, C.B. Sawyer, K.-C. Wang, D.L. White. 2010. The South Carolina Digital

Watershed: end-to-end support for real-time management of water resources. International Journal of Distributed Sensor Networks 2010:1-8.

Fenn, C.R. 1987. Electrical conductivity in Glacio-fluvial Sediment Transfer: An Alpine Perspective. A.M. Gurnell and M.J. Clark (editors). John Wiley and Sons, Chichester, U.K., pp. 377–414.

Flint, K.R. and A.P. Davis. 2007. Pollutant mass flushing characterization of highway stormwater runoff from an ultra-urban area. Journal of Environmental Engineering 133(6):616-626.

Grayson, R.B, C.J. Gippel, B.L. Finlayson, B.T. Hart. 1997. Catchment-wide impacts on water quality: the use of 'snapshot' sampling during stable flow. Journal of Hydrology 199:121-143.

Griffith, Michael B. 2014. Natural variation and current reference for specific conductivity and major ions in wadeable streams of the conterminous USA. Freshwater Science 33(1):1-17.

Glasgow, H.B., J.M. Burkholder, R.E. Reed, A.J. Lewitus, J.E. Kleinman. 2004. Real-time remote monitoring of water quality: a review of current applications, and advancements in sensor, telemetry, and computing technologies. Journal of Experimental Marine Biology and Ecology 300:4009-448.

Hart, J.K., K. Martinez. 2006. Environmental Sensor Networks: A revolution in the earth system science? Earth-Science Reviews 78(3-4):177-191.

Hatt, B. E., T. D. Fletcher, C. J. Walsh, S. L. Taylor. 2004. The influence of urban density and drainage infrastructure on the concentrations and loads of pollutants in small urban streams. Environmental Management 34:1, 112-124

Hem, J.D. 1982. Conductance: A collective measure of dissolved ions. In Water Analysis, Vol. 1. Inorganic Species. R.A. Minear and L.H. Keith (editors). Academic Press, New York, pp. 137–161.

Horrigan, N., S. Choy, J. Marshall, F. Recknagel. 2004. Response of stream macroinvertebrates to changes in salinity and the development of a salinity index. Marine and Freshwater Research 56(6):825-833.

Horrigan, N., J. E. Dunlop, B. J. Kefford, F. Zavahir. 2007. Acute toxicity largely reflects the salinity sensitivity of stream macroinvertebrates derived using field distributions. Marine and Freshwater Research 58:178-186.

Kaushal, S.S., Groffman, P.M., Likens, F.E., Belt, K.T., Stack, W.P., Kelly, V.R., Band, L.E., Fisher, G.T. 2005. Increased salinization of fresh water in the northeastern United States. Proceedings of the National Academy of Science 102:13517-13520.

Kaushal, S.J., S. Duan, T.R. Doody, S. Haq, R.M. Smith, T.A. Newcomer Johnson, K. Delaney Newcomb, J. Gorman, N. Bowman, P.M. Mayer, K.L. Wood, K.T. Belt, W.P. Stack. 2017. Human-accelerated weathering increases salinization, major ions, and alkalinization in freshwater across land use. Applied Geochemistry 83:121-135.

Kaushal, S.J., G.E. Likens, M.L. Pace, R.M. Utz, S. Haq, J. Gorman, M. Grese. 2018. Freshwater salinization syndrome on a continental scale. Proceedings of the National Academy of Science 115(4):3574-E583.

Kotomaki, N. S. Thessler, J. Koshiaho, A.O. Hannukkala, H. Huitu, T. Huttula, J. Havento, M. Jarvenpaa. 2009. Wireless *in-situ* sensor network for agriculture and water monitoring on a river basin scale in southern Finland: evaluation from a data user's perspective. Sensors 9:2862-2883.

Moore, R. D., G. Richards, and A. Story. "Electrical conductivity as an indicator of water chemistry and hydrologic process." Streamline Watershed Management Bulletin 11.2 (2008): 25-29.

Morgan, R.P., K.M. Kline, S.F. Cushman. 2006. Relationships among nutrients, chloride and biological indices in urban Maryland streams. Urban Ecosystems 10(2):153-166.

O'Flynn et al 2010 real time remote monitoring

Paul, M.J. and J.L. Meyer. 2001. Streams in the urban landscape. Annual Review of Ecology and Systematics 32:333-365.

Rose, S. 2002. Comparative major ion geochemistry of Piedmont streams in the Atlanta, Georgia region: possible effects of urbanization. Environmental Geology 42:102-113.

Rose, S. 2007. The effects of urbanization on the hydrochemistry of base flow within the Chattahoochee River basin (Georgia, USA). Journal of Hydrology 341(1-2):42-54.

Sansalone, J.J., J.P. Hird, F.K. Cartledge, M.E. Tittlebaum. 2005. Event-based stormwater quality and quantity loadings from elevated urban infrastructure affected by transportation. Water Environment Research 77(4):348-365.

Sterling, J.L., A.D. Rosemond, S.J. Wenger. 2016. Watershed urbanization affects macroinvertebrate community structure and reduces biomass through similar pathways in Piedmont streams, Georgia, USA. Freshwater Science 35(2): 676-688.

United States Environmental Protection Agency. 1996. National Water Quality Inventory Report to Congress.

United States Geologic Survey. 2020. Groundwater and Streamflow Information Program. https://www.usgs.gov/water-resources/groundwater-and-streamflow-information

Walsh, C. J., A. H. Roy, J. W. Feminella, P. D. Cottingham, P. M. Groffman, and R. P. Morgan II. 2005. The urban stream syndrome : current knowledge and the search for a cure The urban stream syndrome : current knowledge and. Journal of the North American Benthological Society 24:706–723.

Wenger, S. J., A. H. Roy, C. R. Jackson, E. S. Bernhardt, T. L. Carter, S. Filoso, C. A. Gibson, W. C. Hession, S. S. Kaushal, E. Marti, J. L. Meyer, M. A. Palmer, M. J. Paul, A. H. Purcell, A. Ramirez, A. D. Rosemond, K. A. Schofield, E. B. Sudduth, and C. J. Walsh. 2009. Twenty-six key research questions in urban stream ecology: an assessment of the state of the science. Journal of the North American Benthological Society 28:1080–1098.

Wenner, D.B., M. Ruhlman, S. Eggert. 2003. *Proceedings of the 2003 Georgia Water*

Resources Conference, held April 23-24, 2003, at the University of Georgia. Kathryn J. Hatcher, editor, Institute of Ecology, The University of Georgia, Athens, GA 30602.

Wolman, M.G. and A.P. Schick. 1967. Effects of construction on fluvial sediment, urban and suburban areas of Maryland. Water Resources Research 3(2):451-464.